vehicles

MDPI

Article

Mitigating Power Deficits in Lean-Burn Hydrogen Engines with Mild Hybrid Support for Urban Vehicles

Santiago Martinez-Boggio [1], Sebastián Bibiloni [1], Facundo Rivoir [1], Adrian Irimescu [2,*] and Simona Merola [2]

[1] IIMPI—Instituto Ingeniería Mecánica y Producción Industrial, Facultad de Ingeniería, Julio Herrera y Reissig 565, Montevideo 11300, Uruguay; smartinezb@fing.edu.uy (S.M.-B.); sbibiloni@fing.edu.uy (S.B.); frivoir@fing.edu.uy (F.R.)

[2] Science and Technology Institute for Sustainable Energy and Mobility STEMS—CNR, Via G. Marconi 4, 80125 Napoli, Italy; simonasilvia.merola@stems.cnr.it

* Correspondence: adrian.irimescu@stems.cnr.it

Abstract

Hydrogen-fueled internal combustion engines present a promising pathway for reducing carbon emissions in urban transportation by allowing for the reuse of existing vehicle platforms while eliminating carbon dioxide emissions from the exhaust. However, operating these engines with lean air–fuel mixtures—necessary to reduce nitrogen oxide emissions and improve thermal efficiency—leads to significant reductions in power output due to the low energy content of hydrogen per unit volume and slower flame propagation. This study investigates whether integrating a mild hybrid electric system, operating at 48 volts, can mitigate the performance losses associated with lean hydrogen combustion in a small passenger vehicle. A complete simulation was carried out using a validated one-dimensional engine model and a full zero-dimensional vehicle model. A Design of Experiments approach was employed to vary the electric motor size (from 1 to 15 kW) and battery capacity (0.5 to 5 kWh) while maintaining a fixed system voltage, optimizing both the component sizing and control strategy. Results showed that the best lean hydrogen hybrid configuration achieved reductions of 18.6% in energy consumption in the New European Driving Cycle and 5.5% in the Worldwide Harmonized Light Vehicles Test Cycle, putting its performance on par with the gasoline hybrid benchmark. On average, the lean H_2 hybrid consumed 41.2 kWh/100 km, nearly matching the 41.0 kWh/100 km of the gasoline P0 configuration. Engine usage analysis demonstrated that the mild hybrid system kept the hydrogen engine operating predominantly within its high-efficiency region. These findings confirm that lean hydrogen combustion, when supported by appropriately scaled mild hybridization, is a viable near-zero-emission solution for urban mobility—delivering competitive efficiency while avoiding tailpipe CO_2 and significantly reducing NO_x emissions, all with reduced reliance on large battery packs.

Keywords: hydrogen internal combustion engine; lean combustion; mild hybrid electric vehicle; urban mobility

Academic Editor: Dariusz Szpica

Received: 30 June 2025
Revised: 12 August 2025
Accepted: 20 August 2025
Published: 24 August 2025

Citation: Martinez-Boggio, S.; Bibiloni, S.; Rivoir, F.; Irimescu, A.; Merola, S. Mitigating Power Deficits in Lean-Burn Hydrogen Engines with Mild Hybrid Support for Urban Vehicles. *Vehicles* **2025**, *7*, 88. https://doi.org/10.3390/vehicles7030088

1. Introduction

The pursuit of zero-emission mobility has led to increasing interest in hydrogen. Hydrogen-fueled ICEs (H_2-ICEs) offer the potential for carbon-free tailpipe emissions while capitalizing on existing engine architectures, thereby avoiding the full life-cycle environmental impact associated with complete vehicle replacement and taking advantage of the great improvements produced in this technology in the last decade. Hydrogen combustion

primarily produces one compound of concern: nitrogen oxides (NO_x). These emissions are known to be detrimental to both human health [1] and the environment, contributing significantly to air pollution and accelerating climate change [2]. These emissions are most prominent when the engine operates near stoichiometric conditions, typically at high load, where combustion temperatures overpass 2000 K [3]. Operating under lean hydrogen–air mixtures becomes a relevant strategy to mitigate NO_x formation [4,5]. However, a major drawback of lean combustion in H_2-ICEs is the considerable loss in power output [6,7], stemming from hydrogen's inherently low volumetric energy density.

In some cases, effective engine optimization strategies have been shown to partially compensate for this loss, as demonstrated in [8]. This challenge is especially critical in small urban vehicles, where limited engine bay space restricts the extent of possible hardware modifications. Overcoming this power deficit is therefore essential for the successful adoption of hydrogen combustion engines in the light-duty automotive sector, particularly in passenger vehicles, where manufacturers increasingly adopt downsized [9] engines to reduce emissions and fuel consumption without compromising performance [10,11]. An alternative can be the electrification of the powertrain, which involves the integration of a 48 V mild hybrid electric vehicle (MHEV) architecture [12], in which an electric motor assists the engine during transient and low-load conditions. Among the available configurations, P1-type hybrid architectures offer noticeable improvements in both efficiency and performance [13,14], while requiring minimal modifications to the existing internal combustion engine and vehicle layout. This low invasiveness makes them well-suited for real-world retrofitting applications [15]. The reduction in battery size over the vehicle's life cycle, combined with the use of green hydrogen, results in a significantly lower environmental impact compared to a full battery electric vehicle (BEV) [16], particularly in terms of greenhouse gas (GHG) emissions [17]. This is especially relevant in regions where the electricity grid mix is still heavily reliant on fossil fuels, making BEVs more carbon-intensive than ICEVs in certain scenarios [18,19]. The 48 V MHEV system not only compensates for the torque deficit but also improves the overall vehicle efficiency through regenerative braking and by enabling engine operation closer to its optimal efficiency points [20,21]. In a previous work of the research group that authored [15], a mild hybrid 48 V powertrain with a P0 architecture was integrated into a city car retrofitted for stoichiometric hydrogen operation. That study demonstrated how hybridization can compensate for the power deficits typically observed in H_2-fueled engines while also enhancing fuel economy during urban driving cycles. However, the fuel consumption was higher than the gasoline hybrid case.

The lean-burn strategy results in a significant reduction in power output, accompanied by an improvement in thermal efficiency [22,23]; moreover, a notable decrease in undesirable combustion byproducts, particularly NO_x, is observed [8]. This is primarily attributed to the substantial reduction in the in-cylinder peak temperatures, which directly suppress the thermal NO_x formation pathway—governed by the Zeldovich mechanism [24]—due to the lower post-combustion gas temperatures. Lean hydrogen combustion, therefore, emerges as a promising strategy to simultaneously reduce NO_x emissions and enhance thermal efficiency, aligning well with the goals of sustainable propulsion [25]. However, this approach is not without limitations. The lower equivalence ratios significantly reduce the total fuel energy input per cycle, which—combined with hydrogen's already low volumetric energy density—translates into a pronounced drop in indicated torque [26,27]. Moreover, flame propagation is slower under lean conditions, increasing the risk of misfire and incomplete combustion at low loads and engine speeds [28]. These effects are expected to be more critical during cold-start operation, when lower in-cylinder temperatures and a slower mixture preparation further increase the misfire risk. Although cold-start conditions

were not simulated in this work, they represent an important focus for future experimental validation and control strategy development. Lean operation also challenges the robustness of ignition systems, as the required breakdown voltage increases, and even more so with mixture stratification [29]. These issues necessitate careful control of the spark timing, charge motion, and intake conditions to maintain reliable combustion and acceptable drivability. While technologies such as high-energy ignition systems, turbocharging, and EGR dilution control can partially mitigate these challenges, they introduce complexity and costs [30]. Injection studies show that further development is needed for safe and efficient H_2 operation. Comparative analyses of single-hole vs. multi-hole sprays [31] and sensitivity studies on spray–spray impingement confirm that injector design and targeting are critical to stable mixture formation and combustion [29]. As such, integrating lean-burn H_2-ICEs into compact vehicles—especially those retrofitted from conventional architectures—requires complementary strategies to recover lost torque and ensure a dynamic performance that remains competitive with that of conventional powertrains.

The primary objectives of this study were to quantify the impact of lean hydrogen combustion in a small-size passenger car retrofitted with a port fuel injection (PFI) system, and to assess how mild hybridization can compensate for the associated performance losses. To this end, different combinations of engine configurations and battery capacities were evaluated to identify the best trade-off between performance, fuel consumption, and compliance with target driving conditions. A validated 0D/1D engine model was used to simulate lean operation, while the vehicle-level performance was analyzed in GT-SUITE under multiple standardized driving cycles. This dual-modeling approach enabled a comprehensive and integrated analysis of the entire powertrain system. The overarching goal of this research is to determine whether lean H_2 combustion, when combined with mild hybridization, can deliver a viable zero-carbon propulsion strategy for MHEVs, offering a comparable performance and driving range to today's battery-electric vehicles (BEVs) but with significantly reduced dependence on lithium-based energy storage.

2. Materials and Methods

The methodology adopted in this study integrates engine modeling, vehicle simulation, and performance evaluation into a systematic workflow, as illustrated in Figure 1. The process begins with the selection of three engine configurations: a baseline gasoline engine, a hydrogen-fueled engine operating under stoichiometric conditions, and a hydrogen-fueled engine running in ultra-lean mode. Each configuration is modeled numerically using a 0D/1D approach in GT-SUITE, considering thermodynamic and combustion characteristics tailored to each fuel and strategy. The resulting engine models are integrated into a complete vehicle model representing a small city car, where the transient behavior and energy consumption are evaluated under real-world driving cycles. Simulation outputs are then post-processed to extract key performance metrics, such as energy use and engine efficiency, across standardized test procedures. The results are analyzed and compared to assess the feasibility and performance trade-offs of each combustion strategy. The conclusions drawn from this methodology support the development of a conceptual hydrogen hybrid vehicle optimized for urban mobility.

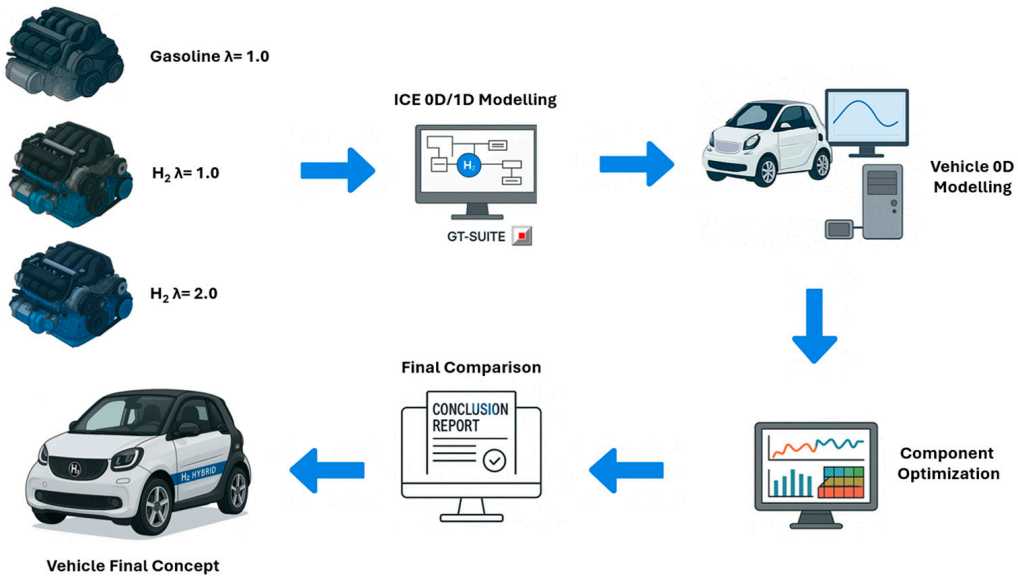

Figure 1. Schematic overview of methodology applied for vehicle performance analysis.

2.1. Engine Modeling and Lean Hydrogen Combustion Strategy

The powertrain under investigation is based on a three-cylinder, turbocharged internal combustion engine originally designed for gasoline fueling. The unit, featuring a total displacement of 599 cm^3, was selected for its relevance in compact urban vehicles. Key characteristics include a bore and stroke of 63.5 mm, a compression ratio of 9.5:1, and a maximum rated output of 40 kW at 5250 rpm. The engine is equipped with a port fuel injection (PFI) system and dual-spark ignition per cylinder. To ensure accurate simulation behavior, a 0D/1D model of the engine was developed in GT-SUITE based on manufacturer specifications and direct physical measurements from a disassembled unit. Details on the engine configuration can be found in Table 1.

Table 1. Technical characteristics of the engine under study.

Parameter	Specification
Engine displacement	599 cm^3
Cylinder configuration	3 in-line cylinders
Intake system	Turbocharged
Fuel delivery	PFI: 3.5 bar (gasoline), 5.0 bar (hydrogen)
Peak output	40 kW at 5250 rpm
Ignition setup	Dual-spark, inductive discharge per cylinder
Bore and stroke	63.5 mm × 63 mm
Compression ratio	9.5:1
Valvetrain	2 valves per cylinder

For hydrogen operation, the base gasoline model was adapted to account for the unique thermodynamic and chemical properties of the fuel. A separate hydrogen injection circuit was implemented in the model, with the appropriate injection pressure and timing adjustments. Due to hydrogen's higher flame speed and wider flammability limits, the ignition timing was recalibrated using a closed-loop controller targeting the maximum brake thermal efficiency. Predictive combustion was handled through the SI Turbulent Flame Combustion Model available in GT-SUITE (see Figure 2), incorporating turbulence and heat transfer effects tailored for lean hydrogen combustion.

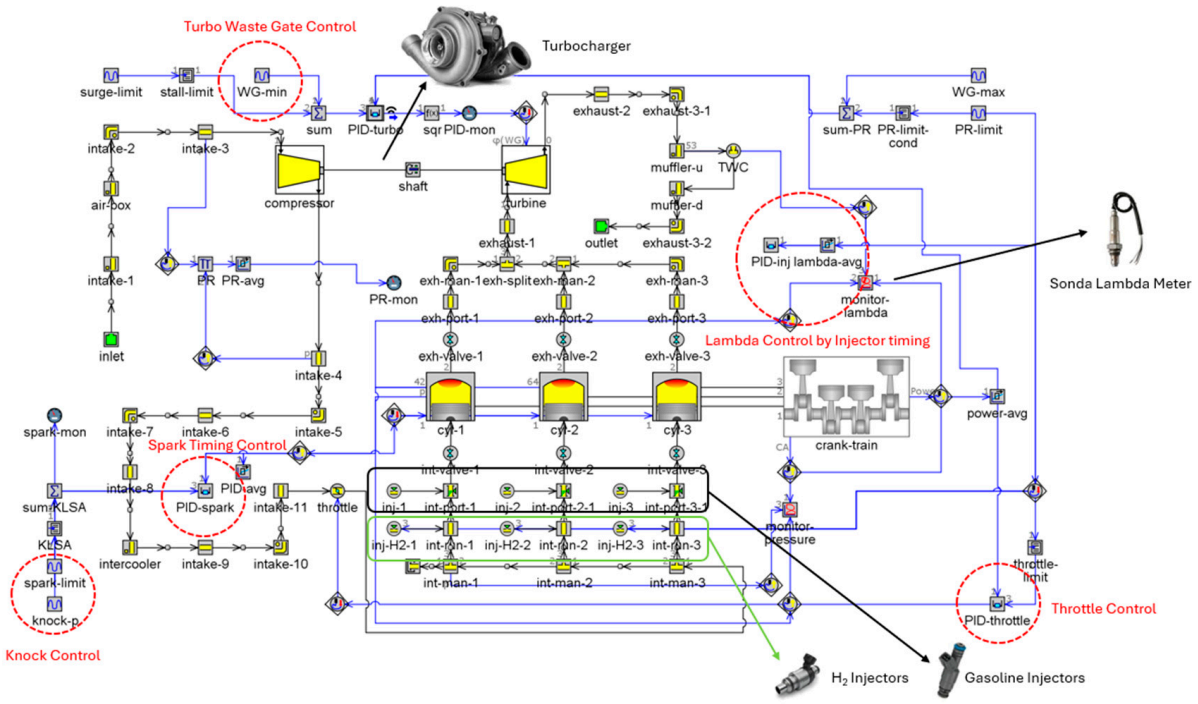

Figure 2. The engine model in GT-SUITE for gasoline and hydrogen injection. The numerical model replicates the behavior of the 600 cm^3 turbocharged engine.

The present study focuses on ultra-lean operation, with global equivalence ratios significantly below stoichiometric levels, aimed at reducing in-cylinder temperatures and suppressing NO_x formation. However, this approach also leads to a diminished indicated mean effective pressure (IMEP), particularly at lower engine speeds. Consequently, maintaining an acceptable performance across the vehicle's operating range necessitates supplemental torque assistance, which is achieved through the integration of a mild hybrid electric system.

Figure 3 shows the resulting maps obtained with the GT-SUITE 1D engine modeling for stoichiometric gasoline operation (baseline), stoichiometric H_2 operation, and lean H_2 operation ($\lambda = 2.0$). In terms of the maximum power output, the engine fueled with hydrogen under stoichiometric conditions achieves performance levels that are remarkably like those observed with gasoline. Across the engine speed range, the maximum power curves of both fuels closely overlap, with differences typically below 1.5 kW. Notably, in the 5000–5500 RPM range, the hydrogen-fueled engine reaches up to 40.01 kW, effectively matching the peak power recorded with gasoline. This suggests that, from a power delivery perspective, operating with stoichiometric hydrogen does not impose a significant performance penalty.

In contrast, under lean hydrogen conditions, the maximum power output is significantly reduced throughout the entire operating range. Compared to gasoline, the observed reductions range from 3 to 17 kW, corresponding to relative losses of 30% to 60%, with the most substantial impact occurring at medium to high loads. This reduction is expected, as highly diluted mixtures inherently limit the achievable charge density and combustion speed, even considering hydrogen's high-flame-speed advantage. In summary, while stoichiometric hydrogen combustion allows the engine to maintain a baseline performance level comparable to gasoline operation, lean-burn hydrogen imposes a considerable constraint on the maximum power output. This trade-off must be carefully evaluated for applications requiring sustained high-load operations or peak performance.

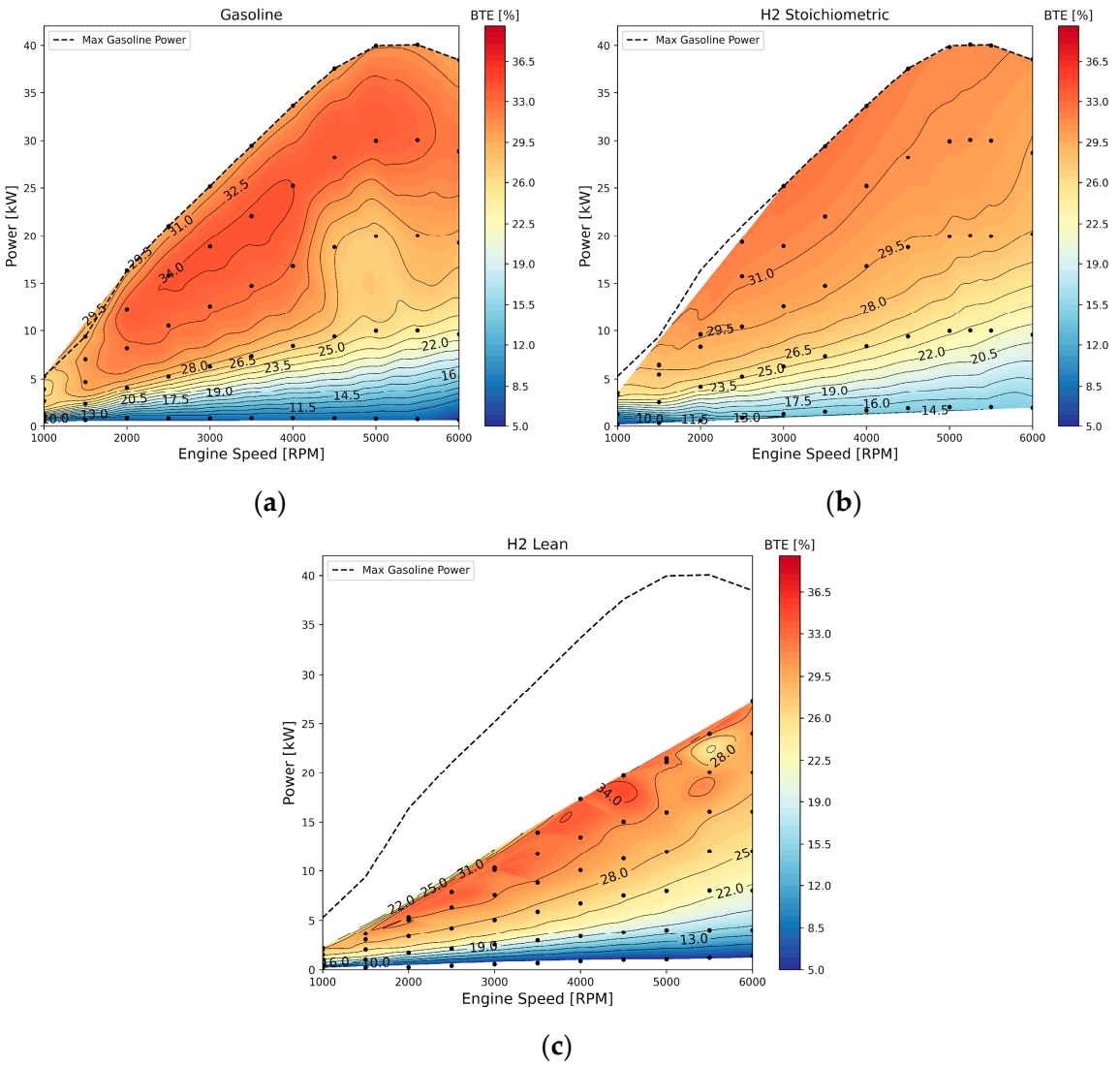

Figure 3. Engine maps obtained by the 0D/1D model with predictive combustion for pure gasoline (**a**), hydrogen with stoichiometric air–fuel ratio (**b**), and hydrogen with lean combustion (**c**).

The brake thermal efficiency (BTE) maps reveal important trends regarding the performance of each fuel and combustion strategy (see Figure 3). The gasoline engine configuration reached a maximum BTE of 34.0%, with an average BTE of 29.6% across the tested operating points. The high-efficiency zone is broad and centered around 3000–4000 RPM and 25–35 kW, indicating well-optimized combustion phasing and energy conversion at moderate to high loads. In contrast, the stoichiometric H_2 configuration achieved a peak BTE of 31.4%, with a mean efficiency of 27.3%. While this mode maintains acceptable efficiency, the high-temperature combustion under stoichiometric conditions limits further gains and increases NO_x formation. Interestingly, the lean hydrogen combustion case achieved the highest BTE overall at 33.2% (it should be noted that the map was limited to the achievable reference torque conditions; for this reason, at high torque demand, lean fueling is limited to lower loads). This reflects the thermodynamic advantage of lean mixtures, which promote lower in-cylinder temperatures and reduce heat losses. The BTE map for lean operation shows localized peaks in efficiency at mid-range speeds and loads; nonetheless, it also reveals a narrower high-efficiency region compared to gasoline. Furthermore, the lean map clearly illustrates the power limitations of this strategy, as the high-efficiency region is confined to lower power outputs, and the efficiency rapidly drops at high loads or very low speeds.

However, the actual fuel consumption and overall efficiency at the vehicle level will strongly depend on how the engine is used during real driving conditions. The operating points selected by the vehicle controller across different driving cycles will determine how much time the engine spends in efficient or inefficient zones. Therefore, vehicle-level modeling is crucial to fully understand the impact of each combustion strategy, especially when assessing performance over standardized or real-world urban cycles. This system-level perspective is essential to accurately evaluate the viability of hydrogen-fueled engines as a zero-carbon propulsion solution.

Although NO_x emissions were not explicitly calculated in this work due to the absence of a fully calibrated NO_x sub-model for hydrogen combustion, the advantages of lean operation in reducing NO_x are well documented in the literature. Ultra-lean mixtures ($\lambda \approx 2.0$) significantly lower in-cylinder temperatures, thereby suppressing the thermal NO_x formation pathway. Studies such as [32,33] consistently report reductions of over 90% in NO_x compared to stoichiometric operation, often approaching measurement limits. Based on these findings [34] and the operating conditions achieved in the simulations of the present work, it is reasonable [35] to expect extremely low NO_x levels for the lean hydrogen cases analyzed in this study.

2.2. Vehicle Model and DoE for Hybrid Powertrain Optimization

A complete vehicle model was developed in GT-SUITE, representing a small two-seater passenger car in its hydrogen-converted configuration (see Figure 4). The hybridization layout corresponds to a P0 mild hybrid architecture, where an electric motor is mechanically coupled to the crankshaft via a belt system. A 48 V lithium-ion battery system serves as the electrical energy source, providing both traction support and regenerative braking capabilities. The P0 configuration offers advantages such as minimal invasiveness, lower cost, and ease of integration into existing vehicle layouts, making it especially attractive for retrofitting conventional platforms to hydrogen operation. Its belt-driven connection to the crankshaft allows the electric motor to assist during acceleration, enables regenerative braking, and supports engine-off coasting without major drivetrain modifications.

However, P0 architectures have inherent limitations compared to P1 and P2 layouts. Because the electric motor is upstream of the transmission, its torque contribution is limited by belt-slip constraints and cannot be multiplied by gearbox ratios. This reduces the ability to provide high torque at the wheels during low-speed operation and limits pure electric propulsion to very short distances. In contrast, P1 configurations—where the motor is mounted directly on the crankshaft—and P2 configurations—where it is placed between the engine and transmission—allow higher torque transfer, improved regenerative efficiency, and more extensive electric-only operation. Nevertheless, these layouts require more complex integration and may involve significant modifications to the transmission or engine housing, making them less practical for cost-sensitive retrofitting projects. In this context, the P0 layout represents the best trade-off between performance gains and implementation feasibility for the present study.

The optimal configuration of the hybrid system was evaluated by a Design of Experiments (DoE) approach based on Latin Hypercube Sampling (LHS). This statistical technique ensures a stratified and space-filling distribution of sampling points across the multidimensional design space while significantly reducing the total number of simulations required. Compared to a full factorial approach—which systematically tests all possible combinations of parameter levels and can become computationally prohibitive as the dimensionality increases—LHS achieves comparable coverage with far fewer simulations by sampling each parameter across its range in a way that avoids redundant combinations.

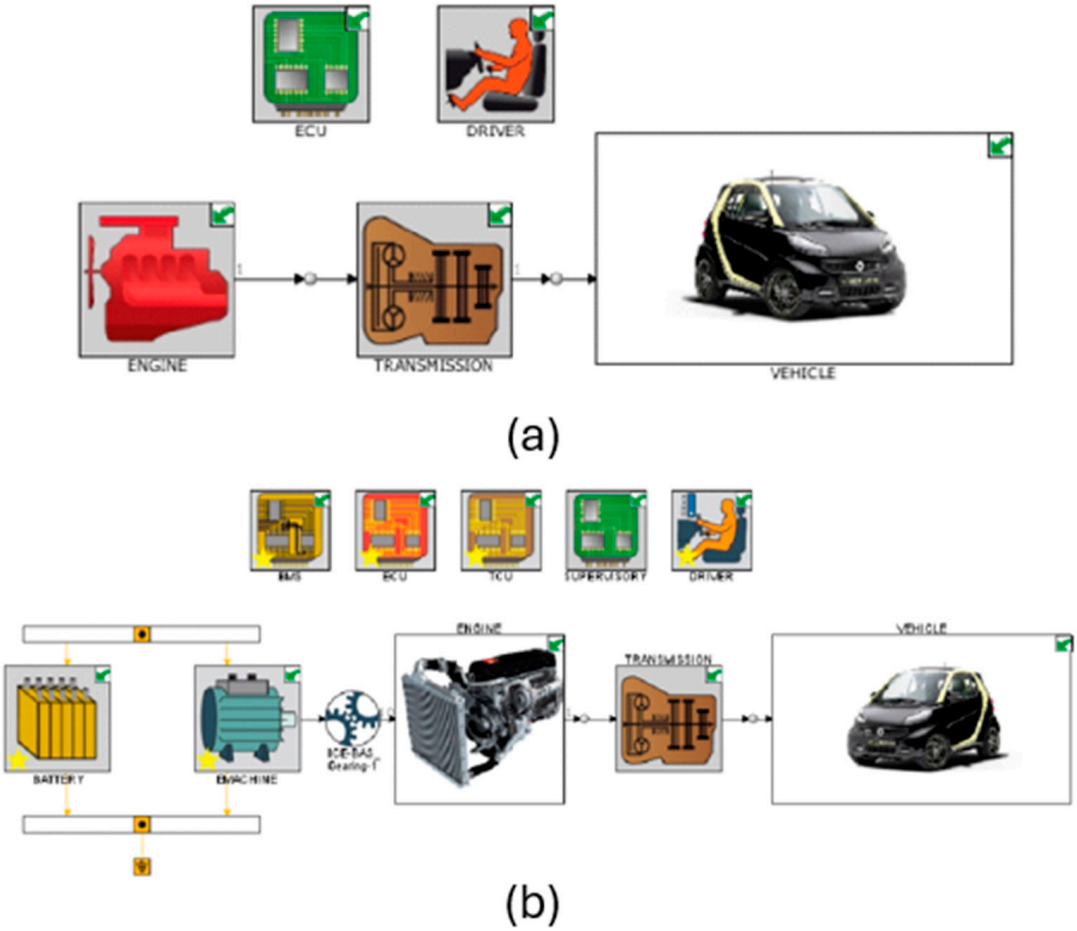

Figure 4. Vehicle model in GT-SUITE for the conventional non-hybrid model (**a**) and the P0 MHEV hybrid model (**b**).

In this study, two primary architectural variables were considered. First, the electric motor sizing varied using torque–speed curves corresponding to continuous power levels from 1 kW to 15 kW, capturing a wide range of possible traction contributions. Second, the battery energy capacity was adjusted by varying the number of parallel cells while maintaining a fixed 48 V nominal voltage, allowing for different combinations of power and energy capabilities while preserving the system's low-voltage design.

Figure 5 presents the distribution of the DoE cases considering two of the six parameters modified in this work: the electric motor power and battery size (expressed as the number of parallel cells). The remaining four parameters, which include RBC control thresholds for torque assistance and hysteresis, as well as gear-shifting strategy coefficients, were also varied. The Latin Hypercube Sampling method ensured a uniform and comprehensive exploration of the multidimensional parameter space.

In the Design of Experiments, the battery capacity and electric motor power were treated as continuous variables to allow for the identification of optimal values without being constrained by current commercial increments. This approach enables a more precise mapping of the design space and avoids overlooking intermediate combinations that could yield better performance. The electric motor size could be varied while maintaining its base efficiency by scaling the maximum torque curve, and the battery capacity could be increased simply by adding more cells in parallel while keeping the nominal voltage fixed at 48 V. While production systems typically adopt discrete component sizes, the continuity assumption is valid at the simulation stage and provides valuable guidance for the subsequent selection of commercially available components.

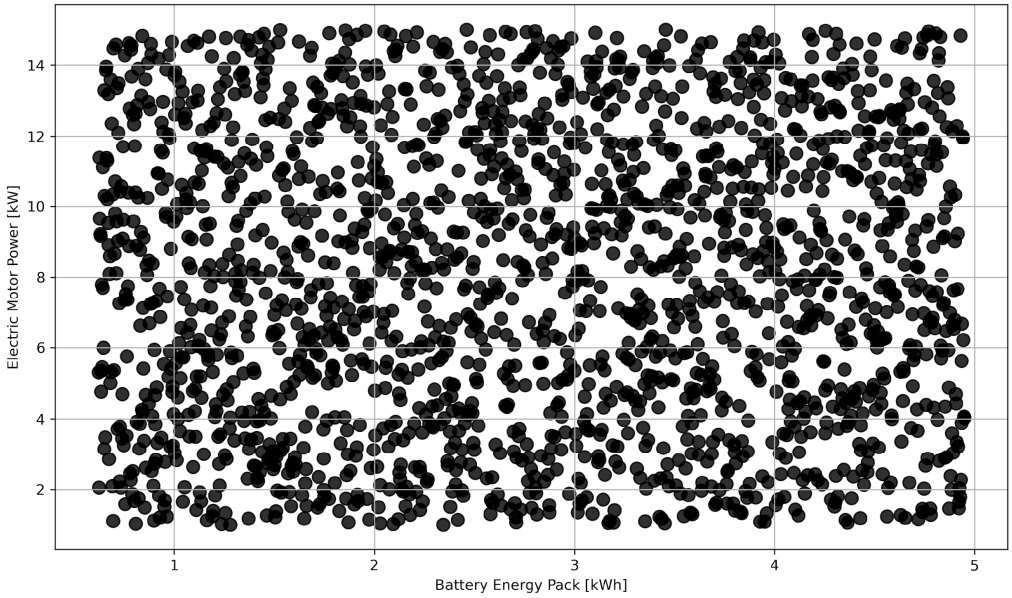

Figure 5. DoE cases for battery and EM using Latin Hypercube Technique.

In parallel, the rule-based control (RBC) strategy managing the energy flow between the engine, electric motor, and battery was refined. The control logic included torque assist activation during low engine loads, regenerative braking during deceleration, and SoC-dependent logic to limit deep discharge or overcharge. An optimization sweep of the RBC parameters was carried out for each configuration to identify control settings that minimize the total energy consumption without compromising performance. A more detailed description of the RBC parameters is presented in Appendix A. The optimal configuration for each case was defined as the one achieving the lowest total energy consumption over the driving cycle. Since the vehicle is not a plug-in hybrid, the evaluation considered not only the fuel energy used during operation but also the net change in the battery state of charge. When the final SOC differed from the initial SOC, the equivalent energy content—converted to the liquid fuel equivalent—was added or subtracted to ensure a fair comparison. This approach ensures that the selected configuration not only matches the best brake thermal efficiency points of the engine but also reflects the true energy demand of the complete powertrain.

Component sizing and control strategy optimization were conducted under the Worldwide Harmonized Light Vehicles Test Cycle (WLTC), the standard homologation procedure, to ensure consistency in the boundary conditions and regulatory relevance. Once the optimal hybrid configurations were identified through WLTC-based simulations, their performance was evaluated across a diverse set of six driving cycles: the New European Driving Cycle (NEDC), the WLTC, Federal Test Procedure 75 (FTP-75), the China Light-Duty Vehicle Test Cycle for Passenger Cars (CLTC-P), the ARTEMIS Urban Driving Cycle, and the New York City Cycle (NYCC), as shown in Figure 6. The chosen set of cycles combines widely used regulatory procedures with real-world urban profiles to ensure both comparability and representativeness. The WLTC and NEDC provide standardized benchmarks for international studies, while FTP-75 and the CLTC-P capture regional traffic characteristics in North America and China, respectively. The ARTEMIS Urban Driving Cycle and NYCC were included to represent highly transient, stop-and-go driving conditions, which are particularly relevant for evaluating the performance of mild hybrid systems and lean hydrogen combustion under demanding urban scenarios. These cycles were selected to capture a broad spectrum of urban traffic dynamics, including varying levels of stop-and-go intensity, acceleration patterns, and average speeds. By analyzing the

energy consumption, battery usage, and engine operating patterns across these cycles, this study highlights how different driving environments influence the hybrid system behavior and overall efficiency, offering insights beyond regulatory test scenarios.

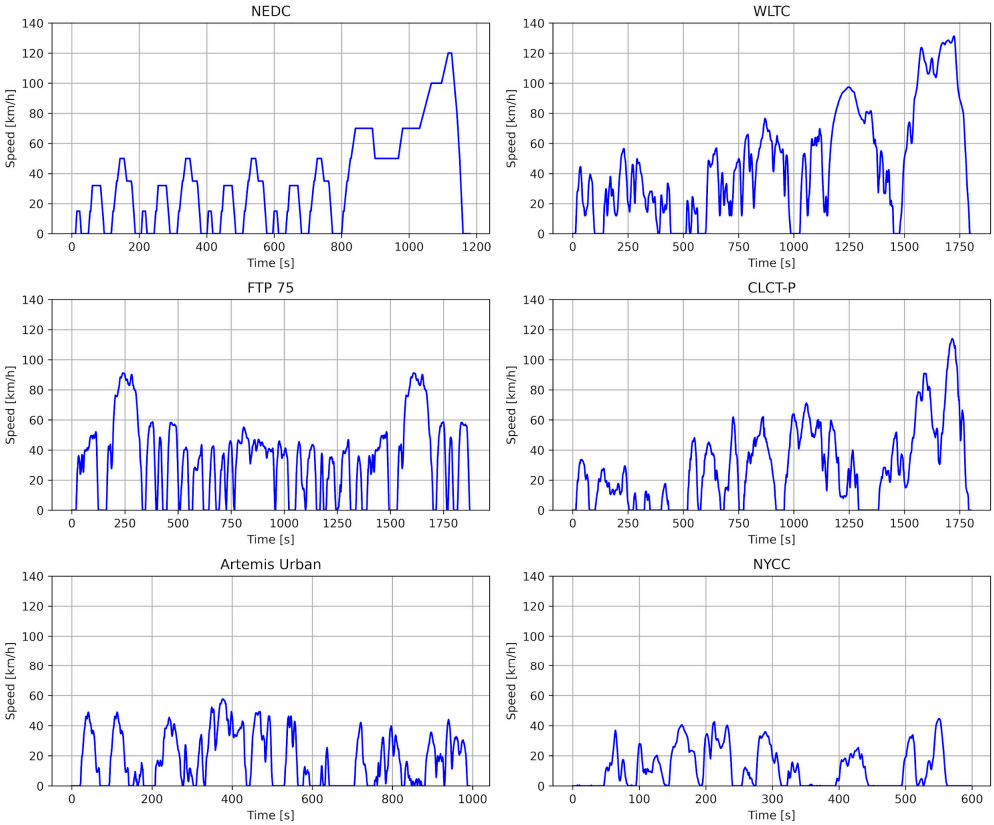

Figure 6. Speed profiles for six standard driving cycles.

3. Results and Discussion

This section presents the outcomes of the component optimization process and the subsequent evaluation of the hybrid powertrain performance across multiple driving conditions. This study first focused on identifying optimal combinations of electric motor powers and battery capacities under the WLTC, the regulatory homologation cycle, using a Latin Hypercube-based Design of Experiments (DoE). These simulations provide a comprehensive understanding of how system sizing influences the energy efficiency across different engine configurations, including gasoline, stoichiometric hydrogen, and lean hydrogen operations. Once the optimal hybrid configurations were determined, their performance was further analyzed under six distinct driving cycles—the NEDC, the WLTC, FTP75, the CLTC-P, ARTEMIS_URBAN, and the NYCC—to assess the real-world behavior, particularly in urban environments. The results not only highlight the efficiency potential of hydrogen-powered hybrids but also emphasize the critical role of vehicle-level integration in determining actual fuel consumption and system effectiveness.

3.1. Component Optimziation

The following analysis explores how hybrid component sizing influences vehicle energy consumption across different fuel and engine configurations. Figures 7 and 8 examine the effects of the electric motor power and battery energy capacity, respectively, using data from a Latin Hypercube-based Design of Experiments under the WLTC. Energy consumption is expressed in kWh per 100 km and is derived by multiplying the fuel volume consumption by the fuel's volumetric energy density. This approach ensures a consistent

comparison between gasoline- and hydrogen-fueled systems, enabling a fair assessment of the impact of electrification on the overall efficiency.

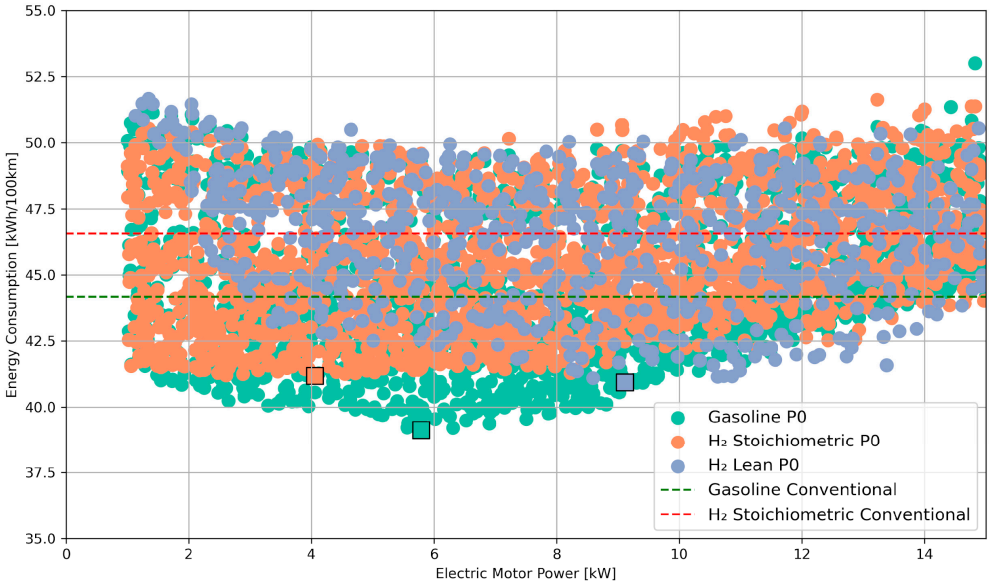

Figure 7. DoE of the electric motor for different engine set-ups under the WLTC.

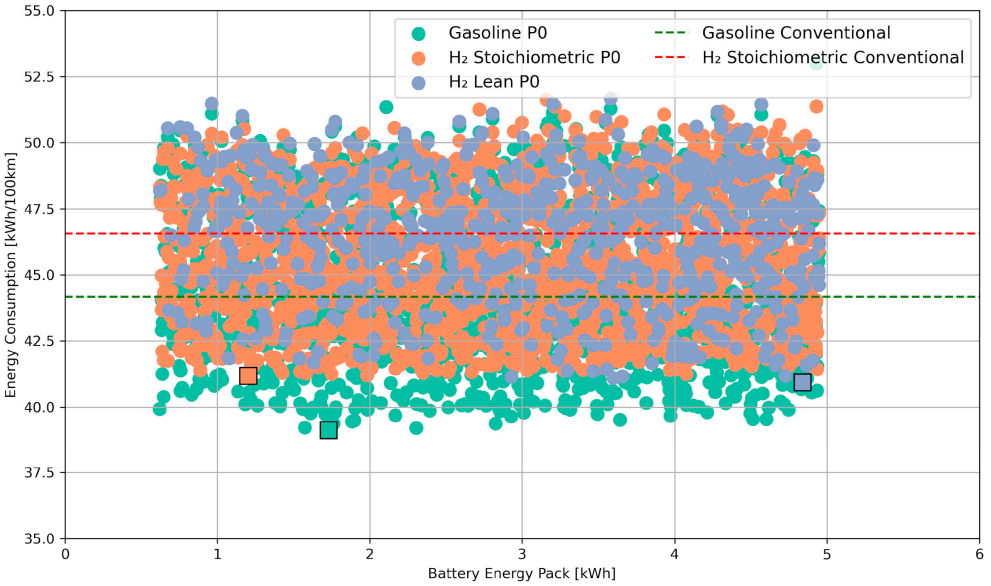

Figure 8. DoE of the battery pack size for different engine set-ups under the WLTC.

Figure 7 presents the results of the DoE on the electric motor sizing for the three P0 hybrid configurations—gasoline, stoichiometric H_2, and lean H_2 —evaluated under the WLTC. The horizontal axis corresponds to the electric motor's continuous power rating (in kW), while the vertical axis shows the resulting vehicle energy consumption in kWh per 100 km. Each dot represents a unique hybrid configuration. For reference, the dashed horizontal lines indicate the energy consumption of the baseline conventional configurations: gasoline (green) and stoichiometric H_2 (red), serving as benchmarks to evaluate the effectiveness of hybridization.

The results reveal distinct trends depending on the fuel type. Gasoline P0 hybrids and hydrogen with stoichiometric calibration achieve substantial reductions in energy consumption with relatively small motors—many configurations under 5 kW already outperform the gasoline baseline. This behavior reflects the fact that, when using the

complete engine map without significant power losses, the benefits of increasing the electric motor size beyond 5 kW become negligible compared to the associated increase in the component weight. Moreover, the potential usage of the electric motor is inherently limited by the P0 mild hybrid architecture, which restricts the extent of the electric torque contribution during high-load transients.

For lean hydrogen configurations, significant energy savings are only achieved once the electric motor size exceeds approximately 9 kW. This threshold marks the point where the hybrid system can effectively compensate for the reduced torque capability of ultra-lean combustion and maintain the engine within its high-efficiency operating regions. Below this level, the electric motor contribution is insufficient to overcome the drivability limitations imposed by lean fueling, leading to energy consumption values consistently above the gasoline benchmark. The best-performing lean H_2 configuration, highlighted by the square marker, confirms that achieving competitive efficiency in this case requires more substantial electrification than for gasoline or stoichiometric H_2 hybrids.

Figure 8 shows the influence of the battery energy capacity on the overall energy consumption for each hybrid configuration. While all configurations benefit to some extent from increasing the battery size, the degree and nature of this benefit vary notably by fuel type. Gasoline P0 hybrids achieve very low energy consumption even with modest battery capacities—below 2 kWh—demonstrating their ability to capitalize on hybrid advantages such as regenerative braking and load shifting with minimal battery sizing. This reinforces their strong synergy with mild hybridization. Stoichiometric H_2 P0 hybrids, in contrast, show relatively high energy consumption throughout the battery size range, with only marginal sensitivity to increased capacity. This suggests that the limitations of stoichiometric hydrogen combustion—particularly under part-load conditions—cannot be substantially mitigated by simply enlarging the battery due to restricted operating efficiency zones and a suboptimal engine response.

Lean H_2 P0 hybrids show the most marked response to increasing battery capacity. Energy consumption drops significantly as the battery size increases, with noticeable improvements beyond 3 kWh. This confirms the battery's essential role in supporting lean hydrogen combustion, particularly in overcoming its lower torque output and helping the engine remain in efficient regions. The best-performing lean configuration, which requires the largest battery among all options (~5 kWh), approaches the energy consumption levels of the gasoline hybrid, underscoring that adequate battery support is critical for lean hydrogen strategies to be competitive.

For comparison, modern mild hybrid electric vehicles typically use very small 48 V battery packs—ranging from 0.4 to 1 kWh in production systems—which suffice for energy recuperation and torque assistance [36]. Some studies have simulated slightly larger packs (e.g., 0.9 kWh in a P2 MHEV context), indicating diminishing returns beyond 1.8 kWh due to thermal limits [37]. In contrast, the lean H_2 hybrid leverages a 5 kWh battery, significantly larger than that of typical MHEV systems, reflecting its key role in compensating for the low-torque delivery inherent to ultra-lean combustion.

From a cost perspective, the P0 lean H_2 MHEV architecture presents both advantages and challenges. On the one hand, the use of an existing internal combustion platform with minimal modifications significantly reduces manufacturing and integration costs compared to fuel cell electric vehicles (FCEVs) or battery electric vehicles (BEVs). The mild hybrid system also requires a smaller battery pack (~5 kWh) than that for BEVs, lowering the lithium demand and associated costs. On the other hand, the high cost of onboard hydrogen storage systems—particularly Type IV composite tanks—remains a major economic barrier, often exceeding the cost of the powertrain itself. Additionally, hydrogen fuel prices per unit of energy are currently higher than gasoline or electricity in most regions. While these

costs are expected to decrease with the scaling of hydrogen production and infrastructure, a full Total Cost of Ownership (TCO) analysis is necessary to quantify the competitiveness of this technology in real-world markets. This will be addressed in future work.

3.2. Vehicle Behaviour

The second stage of the analysis focused on how optimized hybrid configurations perform under diverse operating conditions. Six driving cycles were used to reflect both regulatory testing procedures and representative urban driving scenarios. These cycles differ significantly in terms of average speed, acceleration frequency, and stop–start behavior, offering a comprehensive picture of real-world performance. Results are presented in Figure 9a as absolute energy consumption (kWh/100 km), and in Figure 9b as the percentage difference from each configuration's conventional baseline.

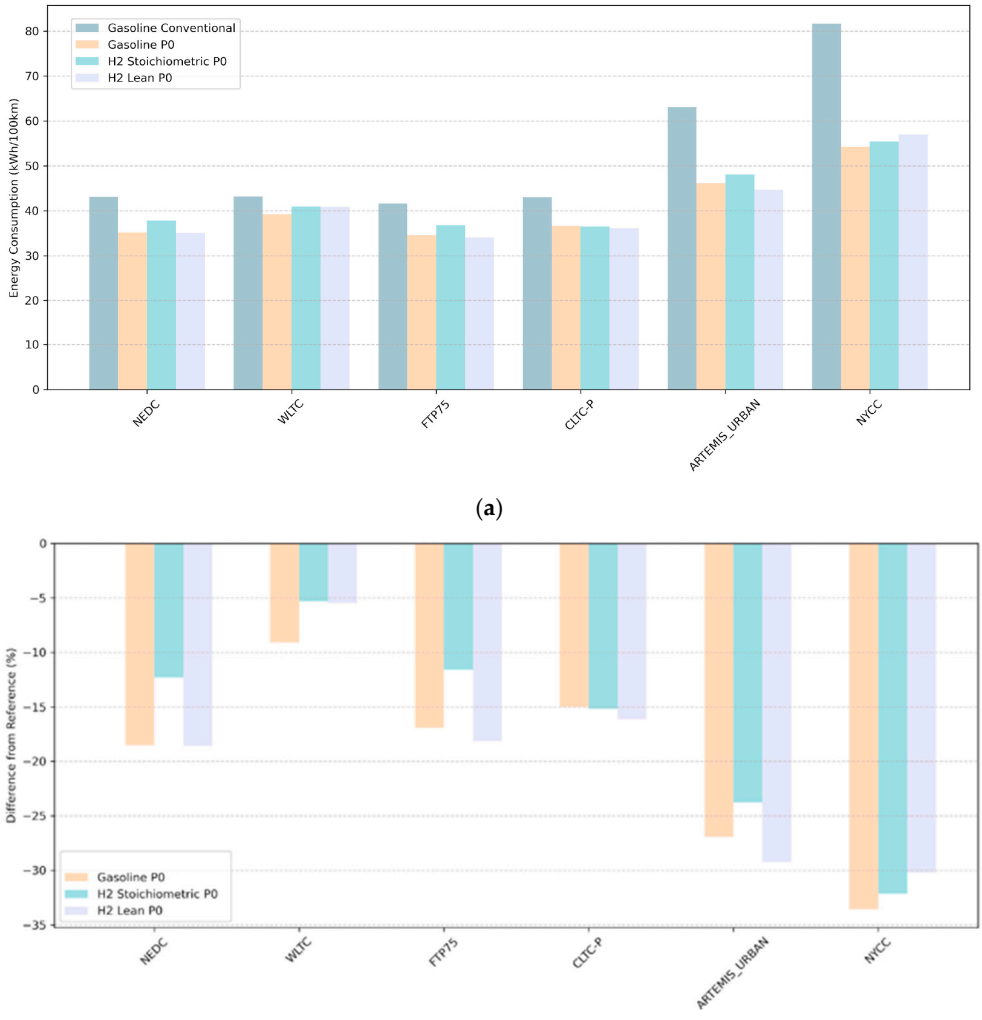

Figure 9. Vehicle powertrain configuration comparison for different driving cycles in terms of energy consumption (**a**) and differences against the gasoline conventional baseline (**b**).

Gasoline P0 hybrids consistently achieved the highest energy savings across all cycles, with reductions ranging from 9.1% in the WLTC to over 33.6% in the NYCC. Particularly large gains were observed in urban-focused cycles with low average speeds and extended idle periods, such as ARTEMIS URBAN (−26.9%) and the NYCC (−33.6%). These results confirm that even mild hybridization significantly enhances energy efficiency in low-load,

stop-and-go conditions by recovering the braking energy and allowing the engine to remain off during idling.

Stoichiometric H_2 P0 hybrids also showed a strong performance across the board, although generally slightly below that of gasoline hybrids. Energy consumption reductions range from 4.6% in the WLTC to 32.1% in the NYCC, with significant gains in ARTEMIS URBAN (−23.8%) and FTP75 (−11.6%). These results indicate that, despite stoichiometric hydrogen combustion's narrower high-efficiency operating window, the integration of mild hybrid support enables meaningful improvements in energy efficiency under urban usage, particularly when electric support is properly scaled. However, the lower part-load thermal efficiency compared to gasoline and lean hydrogen still limits performance under more dynamic acceleration patterns. Lean H_2 P0 hybrids deliver the most balanced and favorable performance among hydrogen-based systems. They achieved energy reductions across all six driving cycles, with the largest improvements observed in the ARTEMIS URBAN (−29.2%), NYCC (−30.2%), NEDC (−18.6%), and FTP-75 (−18.1%). Even in the WLTC and CLTC-P, which include more aggressive accelerations, energy savings remained significant at 5.5% and 16.1%, respectively. These results highlight that the lean combustion strategy, though torque-limited, can achieve high overall efficiency when paired with a properly sized electric motor and battery. The hybrid system helps maintain engine operation within narrow high-efficiency regions and compensates for torque deficits during transients.

In summary, the average energy consumption across the six driving cycles reinforces the conclusions drawn from the individual-cycle analysis. Gasoline P0 hybrids achieved the lowest average consumption at 41.0 kWh/100 km, representing a 22.0% reduction compared to the gasoline conventional baseline of 52.6 kWh/100 km. Lean H_2 P0 configurations follow closely with 41.2 kWh/100 km (−21.5%), while stoichiometric H_2 P0 configurations achieved 42.6 kWh/100 km (−18.9%). Although gasoline hybrids retain a slight advantage, both hydrogen-based hybrids show highly competitive energy performances. Moreover, these results represent a significant improvement over the H_2 conventional (non-hybrid) configuration previously reported by the research group, which exhibited higher energy consumption and poorer performance under transient conditions due to the lack of electrified torque assistance. Beyond energy metrics, the hydrogen-based systems offer key environmental advantages: both eliminate tailpipe CO_2 emissions, and the lean hydrogen strategy, operating at $\lambda \approx 2.0$, is well known to produce extremely low NO_x emissions. Although NO_x was not explicitly modeled in this study, the low-temperature combustion associated with lean hydrogen operation is widely validated in the literature to yield negligible NO_x formation. Thus, the lean H_2 P0 configuration emerges as a technically viable, energy-efficient, and environmentally superior solution for future urban mobility, combining low fuel consumption with near-zero emissions.

Further insight into the underlying causes of energy consumption differences can be gained by analyzing engine operation patterns. Figure 10 presents the engine usage maps for each powertrain configuration under the WLTC, overlaid on their respective BTE contour plots. The red dots indicate actual operating points during the cycle, providing a direct link between vehicle-level control and engine efficiency. In the gasoline conventional case (Figure 10a), the engine operated broadly across the mid- to high-efficiency zones (28–34%), with a dense concentration of points around 2000–3000 rpm and 5–15 kW. However, due to the absence of hybrid assistance, the engine remained active during most low-load phases, leading to suboptimal usage at the lower-efficiency margins of the map.

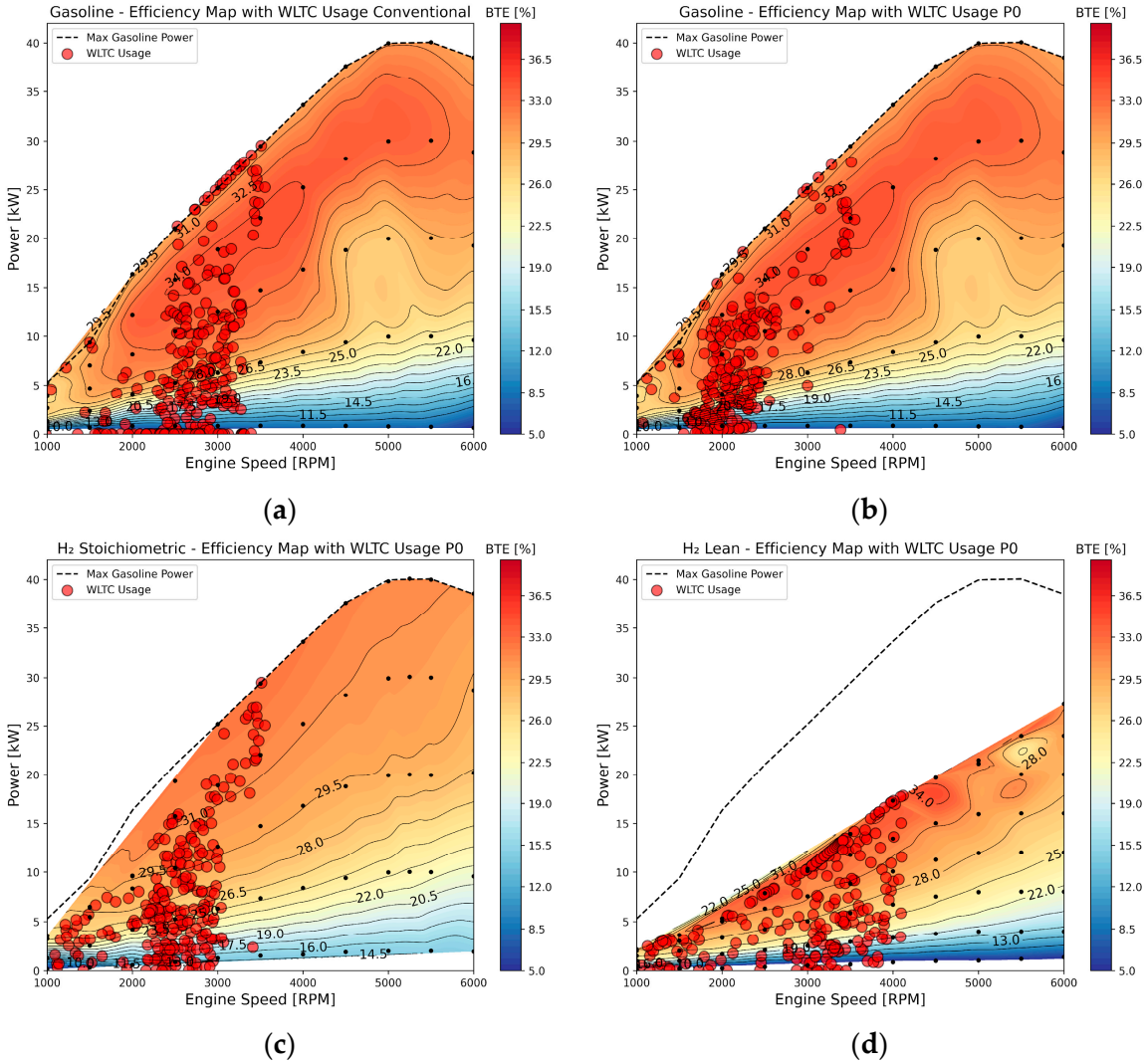

Figure 10. Engine use for gasoline conventional (**a**), gasoline P0 (**b**), stoichiometric H_2 P0 (**c**), and lean H_2 P0 (**d**) in the WLTC.

The gasoline P0 hybrid configuration (Figure 10b) shows a noticeable shift in engine operation. Fewer points are observed in the low-efficiency area below 5 kW, indicating that the hybrid system effectively covers low-load demands using the electric motor. This enables the engine to operate more frequently in regions of higher BTE, increasing the overall efficiency and reducing fuel consumption, as previously shown. In the case of the stoichiometric H_2 P0 configuration (Figure 10c), the usage points are more tightly clustered in the lower-efficiency range (24–30%), particularly below 15 kW and around 2000 rpm. This is a consequence of stoichiometric combustion's narrower optimal zone and lower partial-load efficiency. Even though hybrid control avoids extreme low-load points, the engine's inherent efficiency limitations restrict further gains.

The most distinct operating behavior appears on the lean H_2 P0 map (Figure 10d). Here, the engine operation is heavily concentrated along the narrow band of high-efficiency lean zones (28–33%), with fewer excursions into low-efficiency regions. The map clearly shows that lean operation benefits from sustained mid-load usage, and the hybrid control successfully keeps the engine within this window. However, the restricted torque envelope of lean combustion prevents the engine from supporting higher loads, which may necessitate larger electric contributions.

This usage-based analysis confirms that hybridization allows for the better exploitation of the engine's efficiency potential, but the extent of the benefit varies by fuel. The gasoline hybrid achieves the greatest improvement due to the wide high-efficiency plateau of spark ignition. Lean hydrogen combustion, while less flexible, can be highly efficient if kept within its optimal window—a task for which hybrid control proves especially valuable.

In contrast to the WLTC, the engine usage maps for the New York City Cycle (NYCC) in Figure 11 reveal a markedly different operating behavior. The NYCC is characterized by frequent stops, short acceleration bursts, and low-speed operation, which significantly constrain engine load levels. As shown in Figure 11a, the gasoline conventional setup operates almost exclusively in the low-efficiency region (below 28%), with dense clusters of usage points below 2000 rpm and under 5 kW. This explains the notably high energy consumption observed for this configuration in the NYCC.

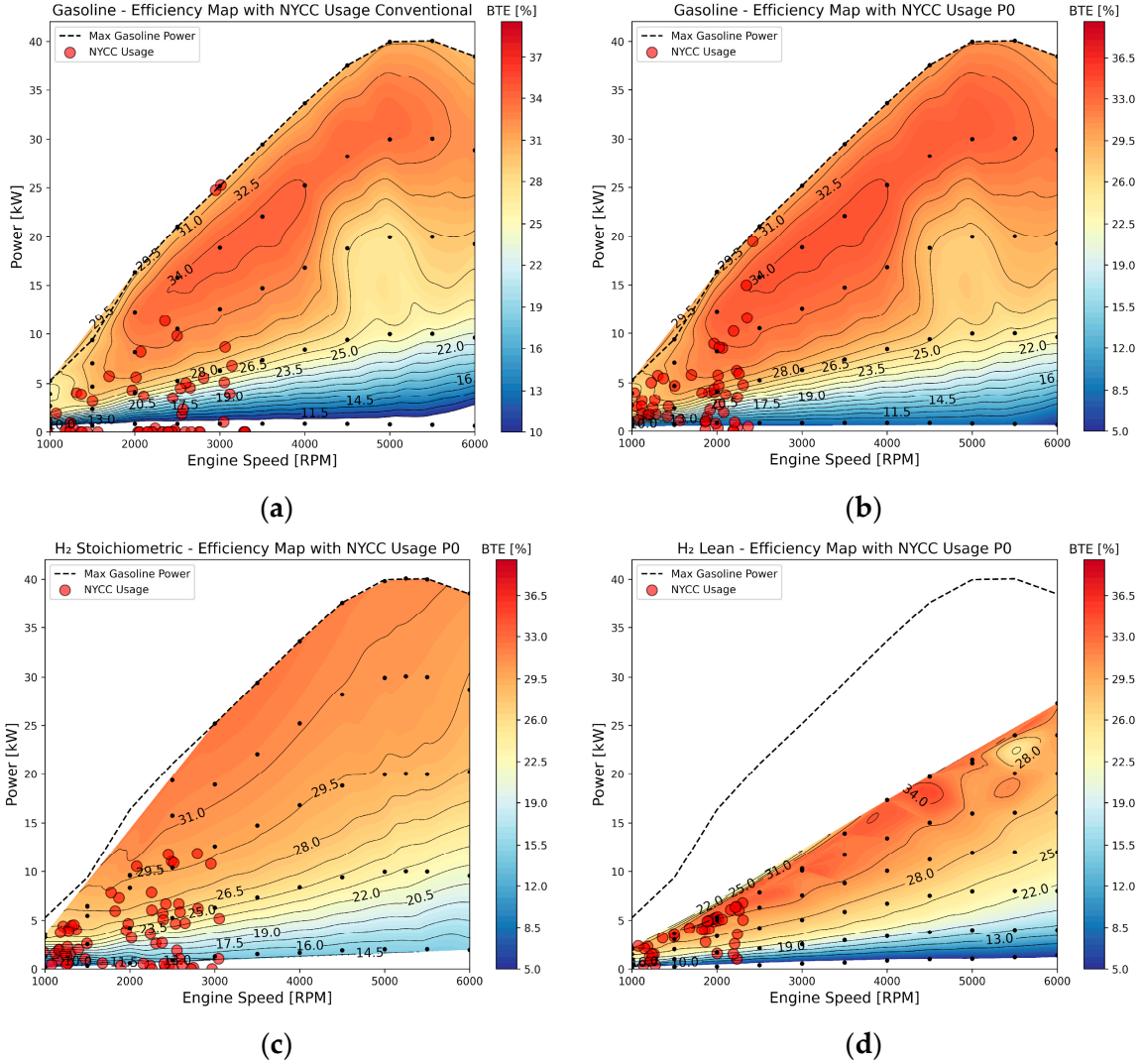

Figure 11. Engine use for gasoline conventional (**a**), gasoline P0 (**b**), stoichiometric H_2 P0 (**c**) and lean H_2 P0 (**d**) in the NYCC.

The gasoline P0 hybrid (Figure 11b) significantly reduces engine usage in these low-efficiency zones. The electric motor effectively absorbs many of the low-load events, allowing the engine to operate less frequently and in more favorable efficiency regions. Although the maximum BTE is not fully exploited due to the NYCC's inherently low power demands, the hybridization yields a tangible improvement in fuel economy, as reflected by a 17% reduction in energy consumption compared to the baseline. For the stoichiometric H_2

P0 configuration (Figure 11c), the engine operates almost entirely in the lower-efficiency range (23–28%) and at very low power levels, highlighting the difficulty of maintaining high efficiency under such transient conditions. The limited flexibility of stoichiometric hydrogen combustion, particularly at low loads, prevents the effective exploitation of the engine's optimal regions, even with hybrid assistance. Figure 11d presents the usage of the lean H_2 P0 powertrain. Despite the inherently better thermal efficiency of lean combustion, the NYCC's low-speed, low-load characteristics constrain engine operation to a narrow band around 2000 rpm and under 10 kW, where the lean BTE is still moderate (25–30%). Although slightly better than the stoichiometric case, the lean configuration does not reach the efficiency levels seen under the WLTC due to the cycle's dynamics.

Overall, these maps demonstrate that urban cycle characteristics profoundly impact engine usage, especially for hydrogen-fueled configurations. While hybridization reduces inefficiencies by offloading low-power demands to the electric motor, the type of fuel and combustion strategy remain critical determinants of efficiency gains. Therefore, understanding and modeling the vehicle behavior across real-world driving conditions is essential for achieving optimal energy performance.

Figure 12 shows an example of the battery SOC behavior and EM vs. ICE power usage by the vehicle in each powertrain configuration. The gasoline P0 case shows a gradual SOC increase during the first part of the cycle, reflecting frequent regenerative braking opportunities and limited electric assistance due to the higher baseline torque capability of the gasoline engine. The stoichiometric H_2 P0 configuration exhibits a relatively stable SOC profile in the early stages, followed by a sustained drop in the latter part of the cycle, indicating greater reliance on EM support to compensate for lower part-load efficiency. The lean H_2 P0 case has the steepest SOC decline after mid-cycle, as the EM is more actively engaged to offset the reduced torque of ultra-lean combustion, especially during medium- to high-load transients.

In terms of the propulsion power, the gasoline P0 shows lower EM utilization peaks and more consistent ICE operation across a wider load range. The stoichiometric H_2 P0 has moderate EM peaks, with the ICE works harder at low-to-mid loads due to narrower high-efficiency zones. The lean H_2 P0 displays the highest EM activity, both in assist and regenerative modes, with the ICE operating within a narrower torque band but requiring more frequent EM intervention to maintain performance targets.

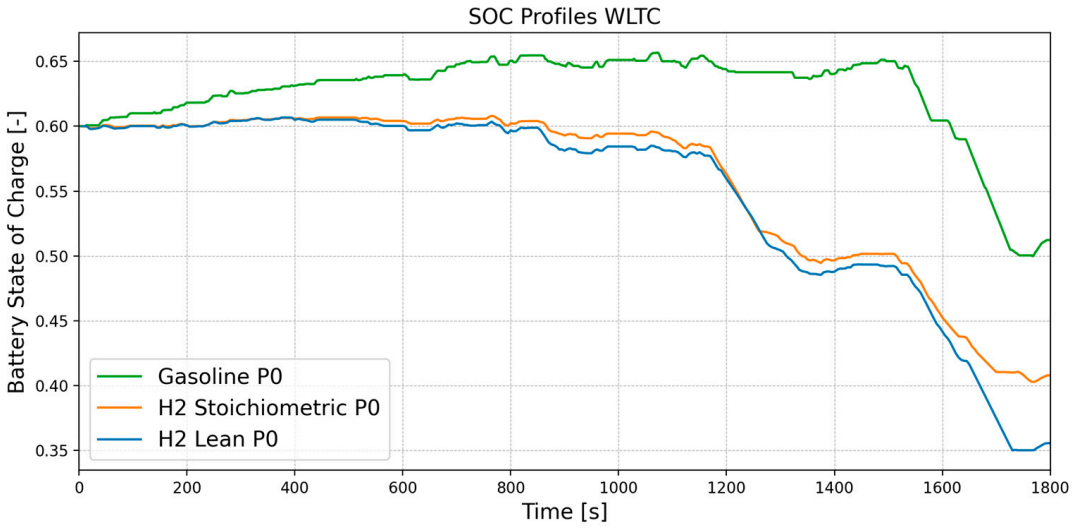

(**a**)

Figure 12. *Cont.*

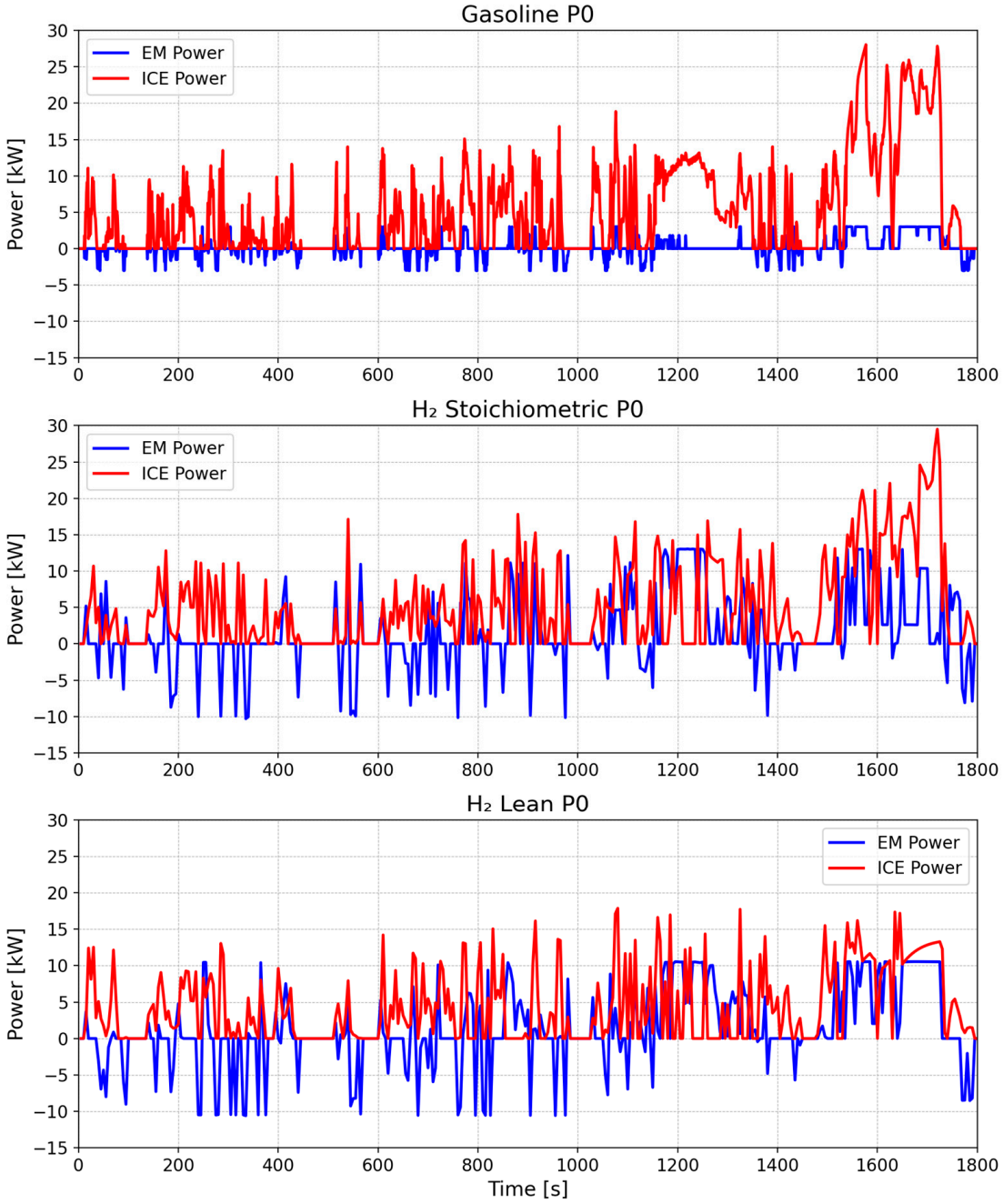

(**b**)

Figure 12. Battery State of Charge (SOC) profiles (**a**) and electric motor (EM) and internal combustion engine (ICE) power profiles for the same configurations (**b**) under the WLTC.

4. Conclusions

This study investigated the viability of lean hydrogen combustion combined with a 48 V mild hybrid system as an alternative propulsion solution for urban vehicles. A validated simulation framework was employed to evaluate the thermodynamic behavior, vehicle-level energy consumption, and performance across multiple standardized and real-world driving cycles. A Latin Hypercube Design of Experiments was used to explore optimal combinations of electric motor power and battery capacity, with a particular focus on lean hydrogen operation.

The results showed that while all configurations benefited from hybridization, the extent of the improvement varied. Gasoline P0 hybrids achieved the greatest average

reduction in energy consumption (−22.0%), followed closely by lean H_2 P0 (−21.5%) and stoichiometric H_2 P0 (−18.9%), compared to the gasoline conventional baseline. In specific driving cycles such as the NYCC and ARTEMIS URBAN, all hybrid architectures delivered strong performances, with lean H_2 matching or outperforming gasoline hybrids in several cases.

The lean hydrogen configuration proved especially effective when supported by an adequately sized electric motor and battery, enabling high brake thermal efficiencies and maintaining operation within optimal efficiency zones across low-speed, stop-and-go cycles. This configuration demonstrated energy consumption as low as 35.1 kWh/100 km in the NEDC and 41.2 kWh/100 km on average across all cycles—comparable to gasoline P0 levels. Moreover, it offers substantial environmental benefits: zero tailpipe CO_2 emissions and negligible NO_x formation due to the ultra-lean combustion strategy ($\lambda \approx 2.0$), as supported by the established literature. These results also highlight a significant improvement over previously studied non-hybrid H_2 configurations, which lacked transient performance and showed higher energy use. The mild hybrid system is thus key to unlocking the full potential of lean hydrogen combustion in compact urban vehicles.

In conclusion, this work demonstrates that lean hydrogen combustion, when integrated into a well-designed 48 V mild hybrid architecture, is a technically and environmentally viable solution for urban mobility. It offers a compelling alternative to battery electric vehicles by reducing reliance on large lithium-ion battery packs while achieving competitive efficiency and near-zero emissions. Future research should target enhanced control strategies for transient conditions, cold-start optimization, and advanced hybrid layouts or forced induction to further improve drivability and broaden the applicability of hydrogen-fueled engines.

Author Contributions: Conceptualization, S.M.-B. and A.I.; methodology, S.M.; software, A.I. and S.M.-B.; validation, S.M.-B., F.R. and S.B.; formal analysis, S.M.-B.; investigation, S.M.-B. and A.I.; resources, A.I. and S.M.; data curation, S.M.-B.; writing—original draft preparation, S.M.-B.; writing—review and editing, S.B., F.R. and S.M.; visualization, S.M.-B.; supervision, A.I. and S.M.; project administration, S.M.-B.; funding acquisition, A.I. All authors have read and agreed to the published version of the manuscript.

Funding: The authors from CNR STEMS acknowledge the funding received within the Turbo48H2 PoC project financed by the European Union—NextGenerationEU (National Sustainable Mobility Center CN00000023, Italian Ministry of University and Research Decree n. 1033—17/06/2022, Spoke 12).

Conflicts of Interest: The authors declare no conflicts of interest. The funders had no role in the design of the study; in the collection, analyses, or interpretation of the data; in the writing of the manuscript; or in the decision to publish the results.

Abbreviations

The following abbreviations are used in this manuscript:

BTE	Brake Thermal Efficiency
CLTC-P	China Light-Duty Vehicle Test Cycle—Passenger
DoE	Design of Experiments
FTP75	Federal Test Procedure 75
GT-SUITE	Gamma Technologies Simulation Environment
ICE	Internal Combustion Engine
LHS	Latin Hypercube Sampling
NEDC	New European Driving Cycle
NO_x	Nitrogen Oxides

NYCC	New York City Cycle
P0, P1	Mild Hybrid Powertrain Configurations (crankshaft-mounted motor architectures)
RBC	Rule-Based Control
WLTC	Worldwide Harmonized Light Vehicles Test Cycle

Appendix A

The mild hybrid electric vehicle (MHEV) system evaluated in this study is governed by a rule-based control (RBC) strategy, implemented within the supervisory controller of the vehicle (Figure A1). This module orchestrates the interaction between the internal combustion engine, electric motor, and battery system, according to driving conditions and system constraints. The RBC logic relies on discrete vehicle modes and logical conditions to dynamically allocate torque between the engine and the electric motor while enabling energy recuperation and optimal use of the battery state of charge.

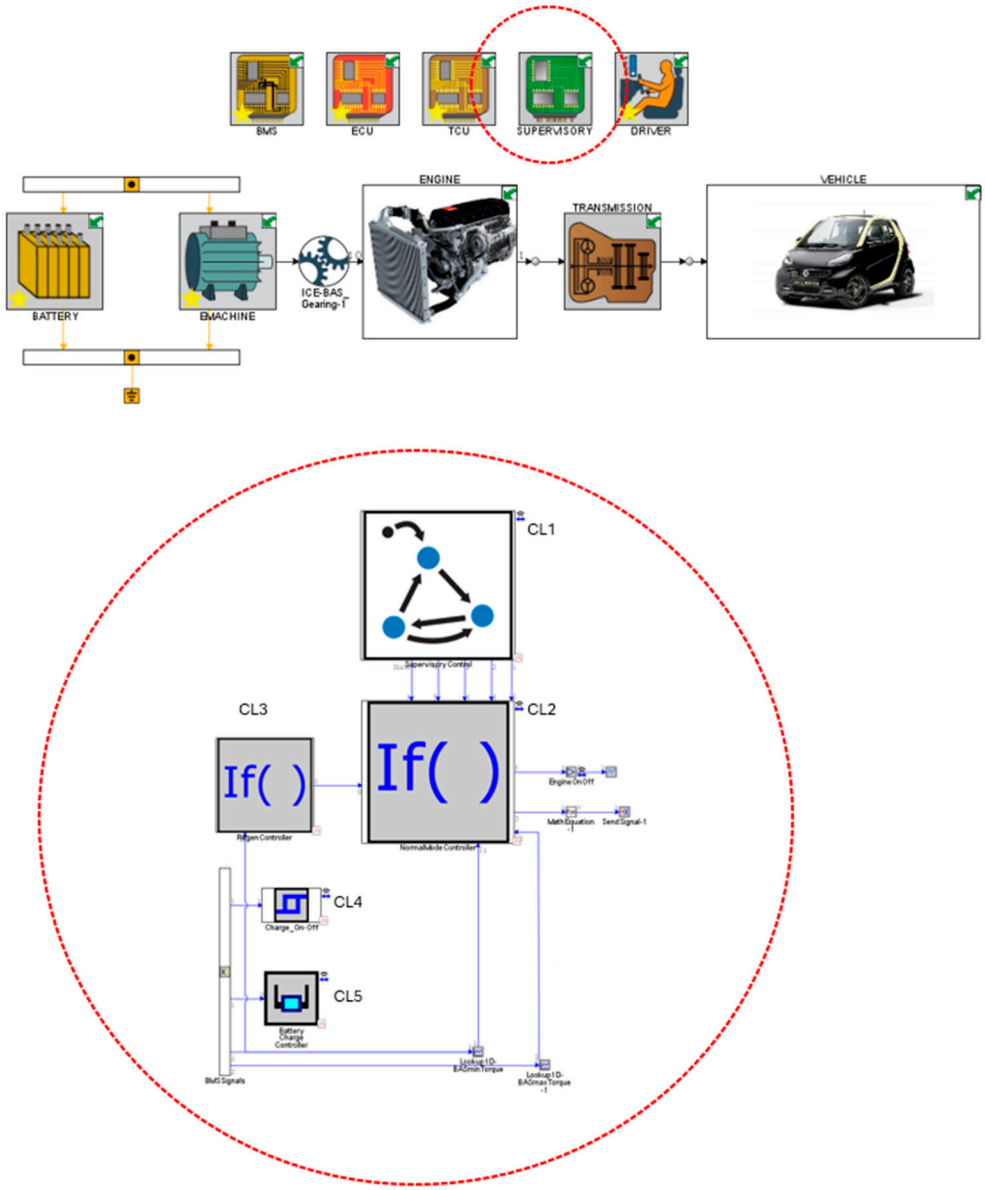

Figure A1. Control scheme of the P0 MHEV. In zoom the supervisory RBC strategy of control.

The control layers can be described as follows:

CL1: Supervisory Mode Control. The vehicle state machine (Figure A1-CL1) defines five operating modes:

1. Engine Off, Vehicle Stopped;
2. Engine Start, Vehicle Stopped;
3. Engine Idle, Vehicle Stopped;
4. Engine Start, Vehicle Moving;
5. Normal Mode.

Transitions between these states are governed by the vehicle speed, driver torque demand, SoC, and regen/load-shift indicators. Once in "Normal Mode," a set of conditional logic blocks determines the exact torque contributions and energy flows based on real-time driving conditions.

CL2: Normal Mode Torque Allocation Logic. The control logic in Normal Mode (Figure A1-CL2) is based on the driver's requested torque, SoC, and other system flags (regen state, charge mode, vehicle speed), and the RBC assigns output values for the following:

- Engine On–Off Status;
- Requested Engine Torque;
- Requested Motor Torque (Engine Equivalent);
- Brake Mode (0 = calculated, 1 = pass driver input);
- Friction Brake Torque (if calculated, Brake Mode == 1).

In low-load conditions, if the SoC is sufficient and the driver demands moderate torque, the electric motor provides torque assistance (maximum EM power), reducing the engine load. During deceleration, if regenerative braking is allowed, the system captures energy through the electric motor; otherwise, friction brakes are used. A mixed-braking mode can also be triggered to split the deceleration torque between regenerative and friction braking in cases where the SoC is high or the power request for braking is higher than the minimum EM power (negative power).

At low speeds, if a load shift is beneficial, the torque demand is shared between the engine and motor to keep the engine within its high-efficiency region. In charge-sustaining operation, the engine provides additional torque to recharge the battery while maintaining drivability. If the driver demands more torque than the engine can provide alone, the motor supplies the excess. At cruising speeds with light loads, the electric motor alone may propel the vehicle. Finally, in standard conditions not matching any special case, the engine supplies the fully requested torque. This hierarchy ensures efficient engine usage, energy recuperation, and smooth transitions between electric and combustion power. When the vehicle is not in "Normal Mode," all actuators are inactive.

CL3: Regenerative Braking Control

The CL3 block governs the activation of regenerative braking based on a set of logical conditions. Using an "If" structure, it evaluates whether regeneration should be allowed. If the battery SoC exceeds 90%, regenerative braking is disabled to avoid overcharging the battery. When braking is requested and the demand exceeds the minimum torque that the electric motor can handle (negative torque threshold), the system either enables full regenerative braking or blends it with friction braking. This logic ensures that energy recuperation occurs efficiently without compromising the battery safety or braking performance. The controller acts as a gatekeeper, enabling regeneration only when conditions are favorable.

CL4: Hysteresis-Based Charge Mode Activation

The CL4 block implements a hysteresis controller to manage transitions into charge-sustaining mode via regenerative breaking from the engine (e.g., in engine load shift or driving-and-charging modes). This avoids frequent toggling between charging and non-charging states, which can lead to unstable or inefficient operation. The controller monitors the SoC and switches the charge mode "on" only when the SoC drops below a defined lower threshold, and it switches it "off" only when it exceeds a higher threshold. When the SoC lies between the thresholds, the output state is held constant. This hysteresis logic helps maintain battery health and smooth powertrain transitions, particularly in cases where engine breaking is used to recharge the battery.

CL5: Battery Charge Control (PID)

The CL5 block includes a simplified proportional control loop (a reduced PID controller) to regulate battery charging during engine-powered modes. The controller compares the actual SoC with a target value (typically initialized at the beginning of the simulation) and generates a proportional torque command to control battery charging through the electric motor. Only the proportional term is used, which scales the torque demand based on the deviation from the target SoC. This ensures that charging actions are scaled appropriately with the battery's needs, avoiding excessive or insufficient charging during normal driving and charge-sustaining phases. This closed-loop approach allows the vehicle to dynamically maintain a healthy battery charge without requiring fixed or time-based charging schedules.

References

1. Boningari, T.; Smirniotis, P.G. Impact of nitrogen oxides on the environment and human health: Mn-based materials for the NO_x abatement. *Curr. Opin. Chem. Eng.* **2016**, *13*, 133–141. [CrossRef]
2. Aryal, B.; Gurung, R.; Camargo, A.F.; Fongaro, G.; Treichel, H.; Mainali, B.; Angove, M.J.; Ngo, H.H.; Guo, W.; Puadel, S.R. Nitrous oxide emission in altered nitrogen cycle and implications for climate change. *Environ. Pollut.* **2022**, *314*, 12027. [CrossRef] [PubMed]
3. Konnov, A.A.; Colson, G.; De Ruyck, J. NO formation rates for hydrogen combustion in stirred reactors. *Fuel* **2001**, *80*, 49–65. [CrossRef]
4. Józsa, V. Mixture temperature-controlled combustion: A revolutionary concept for ultra-low NOX emission. *Fuel* **2021**, *291*, 120200. [CrossRef]
5. Jamrozik, A. Lean combustion by a pre-chamber charge stratification in a stationary spark ignited engine. *J. Mech. Sci. Technol.* **2015**, *29*, 2269–2278. [CrossRef]
6. Malakhov, O.S.; Usatiy, D.Y.; Dyorina, N.V. The Engine Control Unit Improvement for Air-Mixture Control and Engine Power Development. In Proceedings of the 2021 International Russian Automation Conference, Sochi, Russia, 5–11 September 2021; pp. 154–158. [CrossRef]
7. Ran, Z.; Hariharan, D.; Lawler, B.; Mamalis, S. Experimental study of lean spark ignition combustion using gasoline, ethanol, natural gas, and syngas. *Fuel* **2019**, *235*, 530–537. [CrossRef]
8. Wittek, K.; Cogo, V.; Prante, G. Full load optimization of a hydrogen fuelled industrial engine. *Int. J. Hydrogen Energy* **2024**, *77*, 230–243. [CrossRef]
9. Patil, C.; Varade, S.; Wadkar, S. A Review of Engine Downsizing and its Effects. *Int. J. Curr. Eng. Technol.* **2017**, *Special Is*, 319–324. Available online: https://inpressco.com/wp-content/uploads/2017/06/Paper75319-324.pdf (accessed on 22 August 2025).
10. Silva, L.S.; Silva, J.A.; Henríquez, J.R.; de Lira Junior, J.C. Numerical Analysis of Effects of Engine Downsizing and Turbocharging on the Parameters of Performance and Emissions of an Internal Combustion Engine. *Arab. J. Sci. Eng.* **2023**, *48*, 2795–2805. [CrossRef]
11. Fraser, N.; Blaxill, H.; Lumsden, G.; Bassett, M. Challenges for Increased Efficiency through Gasoline Engine Downsizing. *SAE Int. J. Engines* **2009**, *2*, 991–1008. [CrossRef]
12. Liu, Y.; Liao, Y.G.; Lai, M.C. Fuel economy improvement and emission reduction of 48 V mild hybrid electric vehicles with P0, P1, and P2 architectures with lithium battery cell experimental data. *Adv. Mech. Eng.* **2021**, *13*, 1–10. [CrossRef]
13. Yang, Y.; Hu, X.; Pei, H.; Peng, Z. Comparison of power-split and parallel hybrid powertrain architectures with a single electric machine: Dynamic programming approach. *Appl. Energy* **2016**, *168*, 683–690. [CrossRef]
14. Zhang, B.; Shi, P.; Mou, X.; Li, H.; Zhao, Y.; Zheng, L. Energy Management Strategy for P1 + P3 Plug-In Hybrid Electric Vehicles. *World Electr. Veh. J.* **2023**, *14*, 332. [CrossRef]

15. Bibiloni, S.; Irimescu, A.; Martinez-Boggio, S.; Merola, S.; Curto-Risso, P. Mild Hybrid Powertrain for Mitigating Loss of Volumetric Efficiency and Improving Fuel Economy of Gasoline Vehicles Converted to Hydrogen Fueling. *Machines* **2024**, *12*, 35. [CrossRef]
16. Broussely, M. Battery Requirements for HEVs, PHEVs, and EVs: An Overview. In *Electric and Hybrid Vehicles*; Elsevier: North York, NY, USA, 2010; pp. 305–345. [CrossRef]
17. Qiao, Q.; Zhao, F.; Liu, Z.; Jiang, S.; Hao, H. Cradle-to-gate greenhouse gas emissions of battery electric and internal combustion engine vehicles in China. *Appl. Energy* **2017**, *204*, 1399–1411. [CrossRef]
18. Challa, R.; Kamath, D.; Anctil, A. Well-to-wheel greenhouse gas emissions of electric versus combustion vehicles from 2018 to 2030 in the US. *J. Environ. Manag.* **2022**, *308*, 114592. [CrossRef] [PubMed]
19. Liu, Y.; Chen, H.; Li, Y.; Gao, J.; Dave, K.; Chen, J.; Li, T.; Tu, R. Exhaust and non-exhaust emissions from conventional and electric vehicles: A comparison of monetary impact values. *J. Clean. Prod.* **2022**, *331*, 129965. [CrossRef]
20. Oh, H.; Lee, J.; Woo, S.; Park, H. Effect of synergistic engine technologies for 48 V mild hybrid electric vehicles. *Energy Convers. Manag.* **2021**, *244*, 114515. [CrossRef]
21. Benajes, J.; García, A.; Monsalve-Serrano, J.; Martínez-Boggio, S. Optimization of the parallel and mild hybrid vehicle platforms operating under conventional and advanced combustion modes. *Energy Convers. Manag.* **2019**, *190*, 73–90. [CrossRef]
22. Hao, C.; Lu, Z.; Feng, Y.; Bai, H.; Wen, M.; Wang, T. Optimization of fuel/air mixing and combustion process in a heavy-duty diesel engine using fuel split device. *Appl. Therm. Eng.* **2021**, *186*, 116458. [CrossRef]
23. Zhang, M.; Cao, J. Effects of Lean Burn on Combustion and Emissions of a DISI Engine Fueled with Methanol–Gasoline Blends. *Energies* **2024**, *17*, 4023. [CrossRef]
24. Chintala, V.; Subramanian, K.A. CFD analysis on effect of localized in-cylinder temperature on nitric oxide (NO) emission in a compression ignition engine under hydrogen-diesel dual-fuel mode. *Energy* **2016**, *116*, 470–488. [CrossRef]
25. Li, R.; Liu, Z.; Han, Y.; Tan, M.; Xu, Y.; Tian, J.; Yan, J.; Meng, X.; Wei, M.; Hu, S.; et al. Experimental study of the combustion and emission characteristics of ethanol, diesel-gasoline, n-heptane-iso-octane, n-heptane-ethanol and decane-ethanol in a constant volume vessel. *Fuel* **2018**, *232*, 233–250. [CrossRef]
26. White, C.M.; Steeper, R.R.; Lutz, A.E. The hydrogen-fueled internal combustion engine: A technical review. *Int. J. Hydrogen Energy* **2006**, *31*, 1292–1305. [CrossRef]
27. Irimescu, A.; Vaglieco, B.M.; Merola, S.S.; Zollo, V.; De Marinis, R. Conversion of a Small-Size Passenger Car to Hydrogen Fueling: 0D/1D Simulation of EGR and Related Flow Limitations. *Appl. Sci.* **2024**, *14*, 844. [CrossRef]
28. Zhai, C.; Zhang, J.; Li, K.; Dong, P.; Jin, Y.; Chang, F.; Luo, H. Comparative analysis and normalization of single-hole vs. multi-hole spray characteristics: 1st report on spray characteristic comparison. *Green Energy Resour.* **2025**, *3*, 100120. [CrossRef]
29. An, C.; Liu, L.; Luo, H.; Zhou, B.; Liu, Y.; Li, X.; Nishida, K. Threshold sensitivity study on spray–spray impingement under flexible injection strategy for fuel/air mixture evaluation. *Phys. Fluids* **2025**, *37*, 65124. [CrossRef]
30. Gao, J.; Wang, X.; Song, P.; Tian, G.; Ma, C. Review of the backfire occurrences and control strategies for port hydrogen injection internal combustion engines. *Fuel* **2022**, *307*, 121553. [CrossRef]
31. Ricci, F.; Zembi, J.; Avana, M.; Grimaldi, C.N.; Battistoni, M.; Papi, S. Analysis of Hydrogen Combustion in a Spark Ignition Research Engine with a Barrier Discharge Igniter. *Energies* **2024**, *17*, 1739. [CrossRef]
32. Martinez, S.; Irimescu, A.; Merola, S.; Lacava, P.; Curto-Riso, P. Flame Front Propagation in an Optical GDI Engine under Stoichiometric and Lean Burn Conditions. *Energies* **2017**, *10*, 1337. [CrossRef]
33. Martinez, S.; Lacava, P.; Curto, P.L.; Irimescu, A.; Merola, S.S. Effect of Hydrogen Enrichment on Flame Morphology and Combustion Evolution in a SI Engine Under Lean Burn Conditions. In Proceedings of the SAE World 2018, Detroit, MI, USA, 10–12 April 2018; pp. 1–15. [CrossRef]
34. Kosmadakis, G.M.; Rakopoulos, D.C.; Rakopoulos, C.D. Methane/hydrogen fueling a spark-ignition engine for studying NO, CO and HC emissions with a research CFD code. *Fuel* **2016**, *185*, 903–915. [CrossRef]
35. Mehra, R.K.; Duan, H.; Juknelevičius, R.; Ma, F.; Li, J. Progress in hydrogen enriched compressed natural gas (HCNG) internal combustion engines—A comprehensive review. *Renew. Sustain. Energy Rev.* **2017**, *80*, 1458–1498. [CrossRef]
36. Joshi, A. A Review of Emissions Control Technologies for On-Road Vehicles. In *Engines and Fuels for Future Transport*; Springer Nature: Berlin/Heidelberg, Germany, 2022; pp. 39–56. [CrossRef]
37. Basavaradder, A.B.; Dayananda, P.K.; Chethan, K.N. Review on alternative propulsion in automotives -hybrid vehicles. *Int. J. Eng. Technol.* **2018**, *7*, 1311. [CrossRef]